Available online at www.sciencedirect.com

SciVerse ScienceDirect

Procedia Engineering 36 (2012) 360 – 367

Procedia Engineering

www.elsevier.com/locate/procedia

IUMRS-ICA 2011

Effects of Boron and Nitrogen Contents on the Microstructures and Mechanical Properties of Cr-B-N Nanocomposite Thin Films

Jyh-Wei Lee[a,b]*, Chih-Hong Cheng [c], Hsien-Wei Chen[d], Yu-Chen Chan[d], Jenq-Gong Duh[d], Li-Wei Ho[a, *]

[a]*Dept. of Materials Engineering, Ming Chi University of Technology, Taipei 24301, Taiwan, ROC*
[b]*Center for Thin Film Technologies and Applications Ming Chi University of Technology, Taipei 24301, Taiwan, ROC*
[c]*Dept. of Mechanical Engineering, Tungnan University, Taipei,22201, Taiwan, ROC*
[d] *Dept. of Materials Science and Engineering, National Tsing Hua University, Hsin-Chu,30013, Taiwan, ROC*

Abstract

Two series of Cr–B–N nanocomposite thin films with various nitrogen and boron contents were deposited by a co-sputtering process using a bipolar asymmetric pulsed DC reactive magnetron sputtering system, respectively. The crystalline structures and BN bonding nature of thin films were characterized by X-ray diffraction (XRD) and Fourier transform infrared spectroscopy (FTIR), respectively. The cross sectional morphologies of thin films were examined by scanning electron microscopy (SEM) and transmission electron microscopy (TEM). The nanoindentation technique was used to evaluate the hardness and elastic modulus of thin films. The hardness, elastic modulus and H/E ratio increased with increasing nitrogen content, and decreased with increasing boron content. The optimal mechanical properties were achieved on the Cr-3.7 at.% B-54.6 at.% N thin film with a very fine and dense columnar structure.

Keywords: Cr–B–N nanocomposite thin film; FTIR; nanoindentation

1. Introduction

Recently, the boron contained chromium nitride thin films have been explored extensively in the literature [1-6]. It is reported that the nitrogen flow rate ratio during sputtering has strong influence on the phase, microstructure and mechanical properties of the Cr-B-N coating [1-6]. However, the effect of boron content on the phase, microstructure and related mechanical properties of Cr-B-N coatings is seldom studied. In this work, a co-sputtering process using a CrB_2 compound target and a pure Cr target

1877-7058 © 2012 Published by Elsevier Ltd. Open access under CC BY-NC-ND license.
doi:10.1016/j.proeng.2012.03.053

was executed to deposit two series of Cr-B-N thin films containing different boron concentrations and nitrogen contents, respectively, by a pulsed DC magnetron sputtering. Through this process, the influence of boron and nitrogen contents on the phase, microstructure and mechanical properties of Cr-B-N coatings were evaluated.

2. Experimental Structure

The Cr-B-N thin films were deposited on a p-type (100) silicon wafer substrate by a bipolar asymmetry pulsed DC reactive magnetron sputtering system. A pure Cr (99.99 at.%) and a CrB_2 compound target (33%Cr-67%B, in at.%) were placed on the same side of the chamber. The diameter and thickness of each target were 76.2 mm and 6.0 mm, respectively. The substrate was placed between the Cr and CrB_2 targets to deposit Cr–B–N thin films with various boron contents. In the first stage, the different boron contents of Cr–B–N thin films (denoted as series A) were obtained due to the difference of substrate position between the Cr and CrB_2 targets. According to the substrate positions, thin films deposited on Si substrate are denoted as A1 to A7, in which the A1 was close to the Cr target and A7 was close to CrB_2 target. The deposition parameters were listed in Table 1. In the second stage, the nitrogen flow rate was adjusted to deposit Cr-B-N coatings (denoted as series B) with different nitrogen contents. The N_2 flow rate ratios ($N_2/Ar + N_2$), f_{N2}, were set to 8.3%, 25.5%, 33.3% and 41.7%, respectively, and kept at a constant total working pressure of 0.47 Pa. The deposition parameters of the Cr-B-N coatings in second stage are listed in Table 2.

The cross-sectional morphologies of thin films were examined with a field emission scanning electron microscope (FE-SEM, JSM-6701, JEOL, Japan). Selected thin films were further analyzed by TEM to reveal the microstructures in details. Chemical compositions of thin films were analyzed with a field emission electron probe microanalyzer (FE-EPMA, JXA-8500F, JEOL, Japan). The phases of thin films were explored by a glancing angle X-ray diffractometer (XRD, XRD-6000, Shimadzu, Japan) with an incidence angle of 2^o. Cu Kα radiation generated at 30 kV and 20 mA from a Cu target was used. The Fourier transform infrared spectroscopy (FTIR, Spectrum One, Perkin-Elmer, USA) measurement was performed to explore the type of chemical bonds of the BN structure of each Cr-B-N thin film. The FTIR spectrum background of each coating was subtracted from the spectrum of uncoated Si wafer. The hardness and elastic modulus of thin films were investigated by means of a nanoindenter (TI-900, TriboIndenter, Hysitron, USA) using a Berkovich 142.3° diamond probe at a maximum applied load of 3 mN.

Table 1. Deposition parameters of series A coatings.

Sample No.	A1 A2 A3 A4 A5 A6 A7
Cr target power	57 W
CrB_2 target power	150 W
Substrate bias voltage	-149V
Bias frequency	2kHz
Bias Rev. Time	2μs
Bias Rev % voltage	15%
Background pressure	1.6×10^{-3} Pa
Working pressure	0.4 Pa
Coating temperature	250ºC
Input Gas	Ar=6 sccm : N_2=6 sccm

Table 2. Deposition parameters of series B coatings.

Sample No.	B1	B2	B3	B4
Cr target power	30 W			
CrB_2 target power	150 W			
N_2 ratio (%), $N_2/(N_2+Ar)$	8	25	33.3	42
Substrate bias power	4 W			
Substrate bias voltage	-149V			
Bias frequency	2kHz			
Bias Rev Time	2μs			
Bias Rev % voltage	15%			
Background pressure	1.6×10^{-3} Pa			
Working pressure	0.4 Pa			
Coating temperature	250°C			

3. Results and Discussion

3.1. Compositions and crystalline structures of Cr-B-N thin films

The chemical composition of each coating is listed in Table 3. For A series coatings, the boron content increases monotonically from 3.7 at.% (A1) to 20.6 at% (A7), whereas the chromium content decreases from 39.8 at.% (A1) to 20.4 at% (A7). On the other hand, the nitrogen content of each coating is almost the same, which is around 55 at.%. For B series thin films, the nitrogen content increased rapidly with increasing f_{N2} and became saturated at around 53.0 at.% for higher nitrogen gas flow rate, i.e., $f_{N2} > 33.3\%$. In general, the chemical concentrations of chromium and boron decreased with increasing f_{N2}. The X-ray diffraction patterns of series A and B coatings are shown in Fig.1 (a) and (b), respectively. Crystalline CrN phase can be observed for each coating depicted in Fig. 1(a). No XRD signals corresponding to BN and CrB_2 phases are found. The peak intensities decrease and broaden as the boron content of series A coating increases. Clearly, the grain size of Cr-B-N coating in series A decreases with increasing boron content. In Fig. 1(b), the evolutions of peak intensities are strongly influenced by the f_{N2} and nitrogen contents of the films. When a limited amount of nitrogen, $f_{N2} = 8.3\%$ was purged during sputtering, an amorphous-like or extremely fine-scale XRD diffraction pattern was found for the B1 coating. A similar result was also observed for sample B2 as nitrogen content increased to 40.7 at.% and f_{N2} increased to 25.5 %. Meanwhile, very broad XRD peaks corresponding to a CrN phase are obtained for the B3 and B4 coatings, which were deposited at f_{N2} higher than 33.3%. It has been reported that the addition of nitrogen into Cr-B films will induce the nucleation of BN and Cr_xN phases, and thus decrease their grain size dramatically [3]. In this work, the grain refinement effect by boron addition in the Cr-B-N thin film is confirmed.

The FTIR technique was employed to investigate the existence of amorphous BN phase in the coating. According to the FTIR absorption spectrum of series A and B coatings depicted in Figs. 2(a) and (b), respectively, the intensities of h-BN characteristic peaks at 780 cm^{-1} increase with increasing boron and nitrogen contents, indicating the existence of amorphous h-BN phase. Meanwhile, no characteristic peak of c-BN at 1060 cm^{-1} is found [7, 8].

3.2. Microstructure of Cr-B-N thin films

The cross-sectional FE-SEM images of A1, A7, B1 and B3 coatings are shown in Fig. 3(a)-(d), respectively. The thickness of each thin film is around 1000-1100 nm. For the A1 and B1 coatings, very fine columnar structures are revealed. On the other hand, the featureless and glassy microstructures are observed in samples A7 and B3. It is obvious that the addition of boron or nitrogen elements into the Cr-B-N thin film has great influence on the microstructure evolution and alters the microstructure from columnar to featureless.

More details of the microstructures of samples A1, A7 and B3 are revealed by the cross-sectional TEM image as shown in Figs. 4(a)-(c). In Fig. 5(a), very fine columnar structure around 5 nm in width can be found for the A1 coating. On the other hand, the two phases nanocomposite structure consisting of CrN nanograins around 3-4 nm in diameter surrounded by amorphous BN matrix is clearly seen in Figs 4(b) and (c) for A7 and B3 coatings, respectively. Similar results have been reported by Hegedűs et al. [5] on the nanocomposite microstructure of the Cr-B-N thin films deposited at different nitrogen partial pressure.

Table 3. Chemical compositions of all Cr-B-N thin films.

Sample No.	Atomic percentage (at.%)			
	B	Cr	N	O
A1	3.7±0.1	39.8±0.5	54.6±0.7	1.2±0.1
A2	8.1±0.3	34.6±0.2	55.2±0.4	1.4±0.1
A3	11.0±0.8	31.2±0.5	55.2±0.5	1.4±0.1
A4	14.2±0.6	27.6±0.5	55.6±0.4	1.3±0.1
A5	15.7±0.4	26.4±0.5	55.2±0.3	1.4±0.1
A6	20.2±0.3	21.5±0.2	55.7±0.3	1.4±0.1
A7	20.6±0.3	20.4±0.4	56.1±0.6	1.6±0.1
B1	37.9±1.2	43.6±1.5	14.6±2.6	2.7±0.2
B2	18.5±0.3	28.7±0.6	40.7±0.1	12.1±0.3
B3	18.0±0.7	26.1±0.5	52.7±1.3	1.1±0.1
B4	16.9±0.1	25.7±0.2	54.2±0.3	1.1±0.1

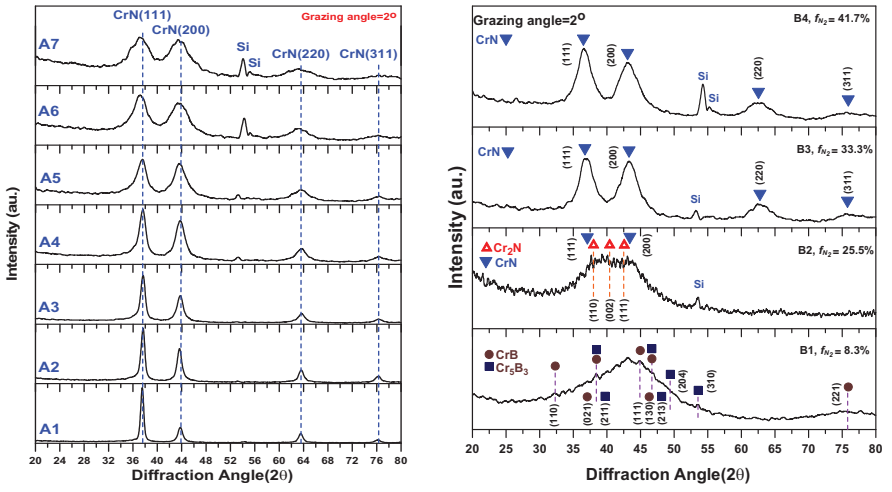

Fig. 1. X-ray diffraction patterns of (a) series A and (b) series B Cr-B-N coatings.

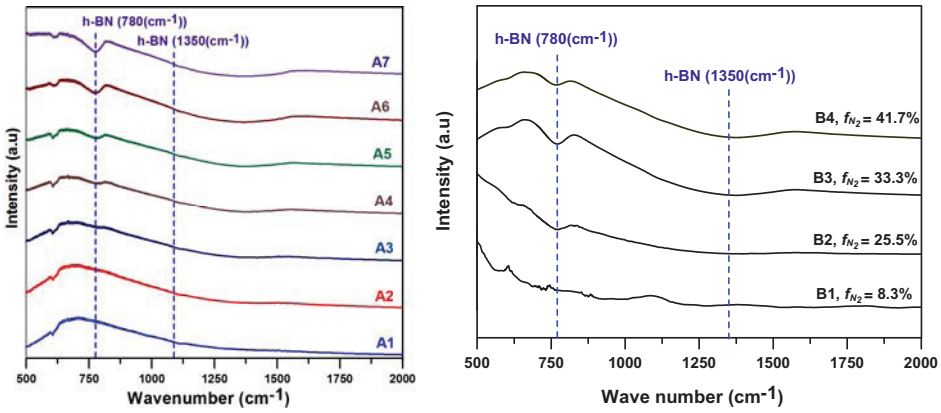

Fig. 2. The FTIR absorption spectra of (a) series A and (b) series B Cr-B-N coatings.

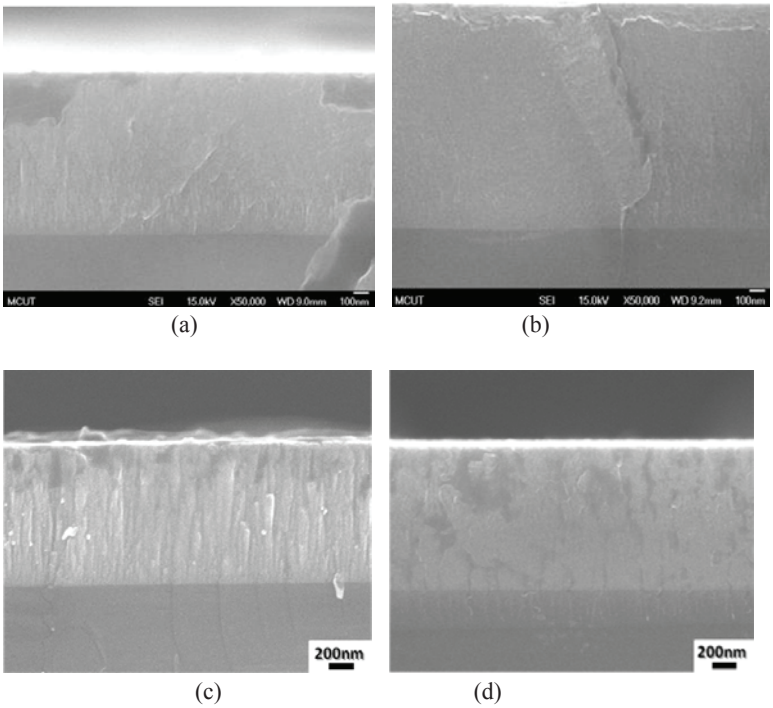

Fig. 3. The cross-sectional SEM morphologies of (a) A1, (b) A7, (c) B1 and (d) B3 coatings.

Based on the microstructure analysis results shown in Figs. 3 and 4, the increasing amounts of boron or nitrogen in the Cr-B-N thin film show a pronounced suppression of columnar growth and thus exhibit a strong nanocomposite structure forming ability.

3.3. Mechanical properties evaluation of Cr-B-N thin films

Figure 5(a) and (b) illustrates the relationships between average hardness, elastic modulus, boron and nitrogen contents for series A and B Cr-B-N thin films, respectively. For the Cr-B-N film containing only 3.7 at.% boron (A1), the highest hardness and elastic modulus around 22 and 210 GPa are obtained due to its dense and fine columnar structure as shown in Fig.4 (a). In addition, the solution hardening effect is also attributed to its higher hardness. It is obvious that the hardness and elastic modulus of series A coatings decreases with increasing boron contents. It is argued that the softening of Cr-B-N film with increasing boron content is caused by the increasing amount of soft amorphous h-BN phase. The lowest hardness and elastic modulus values are observed in the A7 coating, which is possibly attributed to its highest boron concentration (20.6 at.% B) to form the largest volume fraction of soft h-BN phase than other coatings. In Fig. 5(b), the hardness and elastic modulus of B series Cr-B-N coatings decreases with increasing nitrogen content and f_{N2} and then increases again when the nitrogen content is higher than 54.5 at.%, i.e., f_{N2} is higher than 33.3%. The average hardness and elastic modulus reach to 20 and 221 GPa, respectively, for the B4 coating. It is suggested that the softening of the Cr-B-N film with increasing nitrogen content is caused by the soft amorphous BN phase, which is strengthened again by the formation of CrN nanograins and the corresponding nanocomposite structure. In addition, the lowest hardness and elastic modulus values are observed for the B2 coating, which can be possibly attributed to its high B and N contents (21.0 at.% B and 46.3 at.% N) which form the largest volume fractions of the soft amorphous BN phase. The high oxygen contamination for B2 coating due to leakage in the sputter system is another possible reason for its poor mechanical properties. According to the microstructure as shown in Fig. 4(b), it is suggested that the content of soft amorphous BN phase is rather high for the A7 coating, which makes the separation distance between nanograins becomes too large. Accordingly, the nanocrystallites are too small and the intergranular amorphous BN phase is too thick, the resultant hardening effect is thus limited in this work.

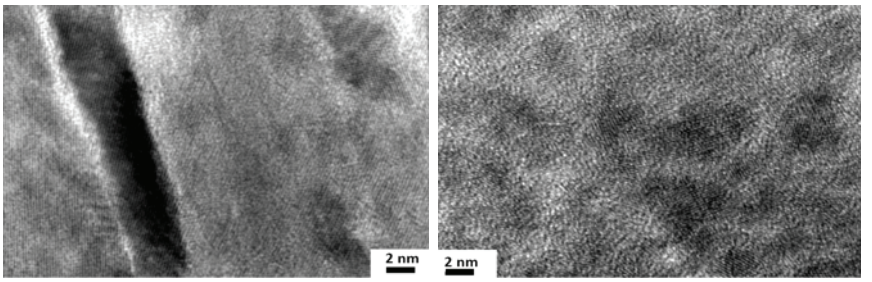

(a) (b)

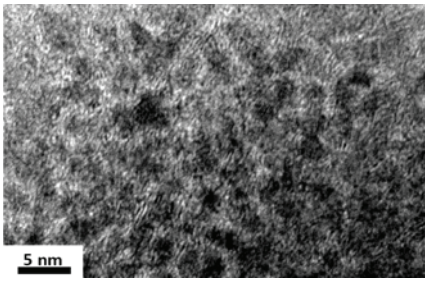

(c)

Fig. 4. The cross-sectional TEM morphologies of (a) A1, (b) A7, and (c) B3 coatings.

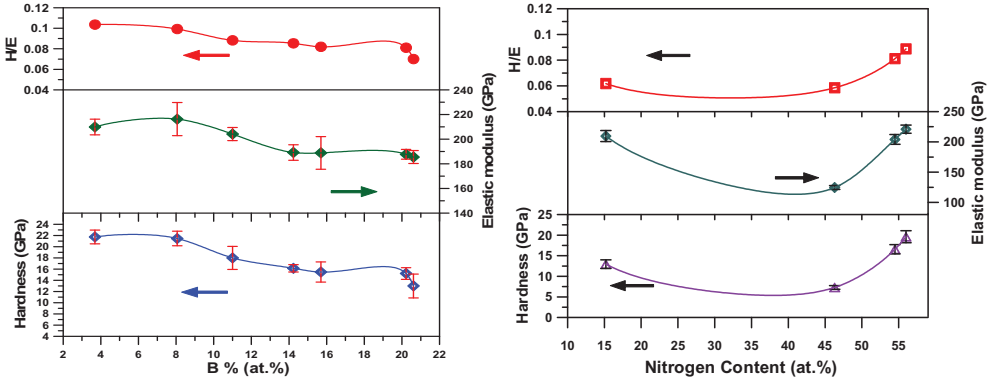

Fig. 5. The relationship between the average hardness, elastic modulus, the H/E ratio and (a) boron and (b) nitrogen contents of Cr-B-N coatings.

Since the H/E ratio is an important factor to describe the resistance of materials against elastic strain to failure [12], the H/E ratio of each coating is also plotted in Fig. 5. In Fig. 5(a) and (b), The tendency for the H/E ratio with respect to the boron or nitrogen contents is almost the same as compared with those of hardness and modulus. Finally, It can be concluded that the A1 coating containing Cr-3.7 at.%B-54.6 at.% N exhibits the optimal mechanical properties due to its fine columnar structure in this work.

4. Conclusions

In this work, two series of Cr–B–N thin films containing various boron and nitrogen concentrations were investigated. The amount of amorphous h-BN phase increased with increasing boron and nitrogen contents based on the FTIR analysis. It can be concluded that the boron and nitrogen elements showed strong influence on the microstructure and mechanical properties of Cr-B-N thin films. The hardness, elastic modulus and H/E ratio increased with increasing nitrogen content. On the other hand, the hardness, elastic modulus and H/E ratio decreased with increasing boron content, which was possibly attributed to the microstructure of Cr-B-N coatings containing small nanocrystallites and thick intergranular amorphous BN phase. The optimal mechanical properties were achieved on the fine columnar structured Cr-3.7 at.% B-54.6 at.% N thin film.

Acknowledgements

The authors gratefully acknowedge the financial support of the National Science Council of Taiwan, ROC through contracts No. NSC 99-2221-E-131-043 and NSC 100-2221-E-131-008- MY3.

References

[1] Mitterer C. Borides in thin film technology. *J Solid State Chem* 1997; 133:279-291.
[2] Aouadi SM, Namavar F, Tobin E, Finnegan N, Haasch RT, Nilchiani R, Turner JA, Rohde SL. Characterization of CrBN films deposited by ion beam assisted deposition. *J Appl Phys* 2002;91:1040.
[3] Gorishnyy TZ, Mihut D, Rohde SL, Aouadi SM. Physical and mechanical properties of reactively sputtered chromium boron

nitride thin films. *Thin Solid Films* 2003; **445:96**-104.

[4] Kiryukhantsev-Korneev PhV, Pierson JF, Petrzhik MI, Alnot M, Levashov EA, Shtansky DV. Effect of nitrogen partial pressure on the structure, physical and mechanical properties of CrB_2 and Cr–B–N films. *Thin Solid Films* 2009; **517**:2675-2680.

[5] Hegedűs É, Kovács I, Pécz B, Tóth L, Budna KP, Mitterer C. Transmission electron microscopy of nanocomposite Cr–B–N thin films. *Vacuum* 2008; **82:209**-13.

[6] Budna KP, Mayrhofer PH, Neidhardt J, Hegedűs É, Kovács I, Tóth L, Pécz B, Mitterer C. Effect of nitrogen-incorporation on structure, properties and performance of magnetron sputtered CrB_2. *Surf Coa Technol* 2008;**202**:3088-3093.

[7] Budak E, Bozkurt C. Synthesis of hexagonal boron nitride with the presence of representative metals. *Physica B* 2010; **405:4702**.

[8] Xin H, Shi X, Lin C, Xu W, Zhong L, Zou S. Phase evolution in boron nitride thin films prepared by a dc-gas discharge assisted pulsed laser deposition. *Thin Solid Films* 1997; **293**:17-21.

[9] Leyland A, Matthews A, On the significance of the H/E ratio in wear control: a nanocomposite coating approach to optimised tribological behaviour. *Wear* 2000;**246**:1-11.